JOURNAL OF SPACECRAFT AND ROCKETS
Vol. 48, No. 3, May–June 2011

Vacuum Ultraviolet/Atomic Oxygen Erosion Resistance of Amorphous $Si_{0.26}C_{0.43}N_{0.31}$ Coating

L. F. Hu,* M. S. Li,† J. J. Xu,* Ziqi Sun,* and Y. C. Zhou‡
Chinese Academy of Sciences, 110016 Shengyang, People's Republic of China

DOI: 10.2514/1.38391

An amorphous silicon carbonitride ($Si_{1-x-y}C_xN_y$, $x = 0.43$, $y = 0.31$) coating was deposited on polyimide substrate using the magnetron-sputtering method. Exposure tests of the coated polyimide in atomic oxygen beam and vacuum ultraviolet radiation were performed in a ground-based simulator. Erosion kinetics measurements indicated that the erosion yield of the $Si_{0.26}C_{0.43}N_{0.31}$ coating was about 1.5× and 1.8 × 10^{-26} cm^3/atom during exposure in single atomic oxygen beam, simultaneous atomic oxygen beam, and vacuum ultraviolet radiation, respectively. These values were 2 orders of magnitude lower than that of bare polyimide substrate. Scanning electron and atomic force microscopy, X-ray photoelectron spectrometer, and Fourier transformed infrared spectroscopy investigation indicated that during exposures, an oxide-rich layer composed of SiO_2 and minor Si-C-O formed on the surface of the $Si_{0.26}C_{0.43}N_{0.31}$ coating, which was the main reason for the excellent resistance to the attacks of atomic oxygen. Moreover, vacuum ultraviolet radiation could promote the breakage of chemical bonds with low binding energy, such as C-N, C = N, and C-C, and enhance atomic oxygen erosion rate slightly.

Nomenclature

A	=	exposed area of materials, cm^2
E_y	=	erosion yield of materials, cm^3/atom
F	=	atomic oxygen flux, atoms/cm^2 s
t	=	exposure time, s
ΔM	=	mass loss of materials, g/cm^2
ρ	=	density of materials, g/cm^3

I. Introduction

IN LOW-EARTH-ORBIT (LEO) space, highly reactive atomic oxygen (AO) can cause severe damages of polymer materials, such as mass loss and changes in optical, mechanical, electrical, and chemical properties [1,2]. For most widely used polymers or polymer-based composites, such as polyimide, their AO erosion yield is in the order of 10^{-24} cm^3/atom [3]. In LEO, vacuum ultraviolet radiation (VUV) also results in degradation of these polymer materials. It has been identified that AO is the most important factor for degradation of space materials. In the coexistence of AO and VUV radiation, AO attacks become more serious [4–6].

To improve AO resistance of space materials, various protective coatings have been developed, including organic coatings (silicones, fluoropolymers) [7], inorganic coatings (Al_2O_3, SiO_2) [8], and organic/inorganic hybrid coatings (so-called ceramers) [9,10]. Among these coatings, organic and organic/inorganic coatings have an enhanced AO erosion resistance, good flexibility, and simple processability. However, these two kinds of coatings may be susceptible to VUV radiation and space debris collision. On the contrary, inorganic coatings can provide excellent AO protection, are very stable under VUV radiation. But this kind of coatings cracks and fails easily due to their intrinsic brittleness. To solve this shortcoming of inorganic coatings, fine grain coatings and multilayer coatings with self-healing capability were proposed [11]. Meanwhile, it is still necessary to develop new inorganic coating systems with good cracking resistance.

Recently, the Si-C-N system has drawn immense interest due to its excellent chemical and mechanical properties [12,13]. In oxidative environments, $Si_{1-x-y}C_xN_y$ shows good oxidation resistance due to the formation of an entire oxide layer. The toughness of $Si_{1-x-y}C_xN_y$ is 3.5 MPa $m^{1/2}$ [14], being greater than that of traditional oxides, such as SiO_2 (1.0 MPa $m^{1/2}$) and Al_2O_3 (2.7 MPa $m^{1/2}$).§ Therefore, the $Si_{1-x-y}C_xN_y$ coating may display low crack tendency during handling or loading, which may endow itself better AO resistance than traditional inorganic coatings. On the other hand, the brittleness of the $Si_{1-x-y}C_xN_y$ can be further improved by preparation of polymeric method or adjusting its structure [15]. As a result, it is potential for applications as AO resistant coating. However, there are few reports about AO or VUV/AO resistance of $Si_{1-x-y}C_xN_y$ coatings.

In the present work, an amorphous $Si_{1-x-y}C_xN_y$ ($x = 0.43$, $y = 0.31$) coating was deposited on polyimide substrate using magnetron-sputtering method. Subsequently, the protectiveness of the $Si_{0.26}C_{0.43}N_{0.31}$ coating was evaluated by AO/VUV exposure tests in a ground-based LEO simulator. The VUV effects on AO erosion of the $Si_{0.26}C_{0.43}N_{0.31}$ coating were investigated.

II. Experimental Details

$Si_{1-x-y}C_xN_y$ coatings were prepared using a magnetron sputtering system by reactive cosputtering two targets of silicon (purity 99.99%) and graphite (purity 99%) in Ar/N_2 with a dc mode. The contents of Si and C in $Si_{1-x-y}C_xN_y$ coating were adjusted by varying the power density of Si and C targets, respectively. The setup of these two targets is illustrated schematically in Fig. 1. Before deposition, the polyimide substrate was cleaned with acetone and methanol, and rinsed with de-ionized water, finally dried with clear air. By adjusting the deposition conditions, $Si_{1-x-y}C_xN_y$ coatings with different Si, C, and N content could be obtained. In this study, a $Si_{1-x-y}C_xN_y$ coating deposited with high Si/C power ratio was selected for exposure test due to its dense and uniform structure [15]. The corresponding deposition conditions of this coating are listed in Table 1.

Surface compositions of the as-deposited $Si_{1-x-y}C_xN_y$ coatings were determined by X-ray photoelectron spectrometer (XPS)

Received 4 May 2008; revision received 7 July 2009; accepted for publication 18 January 2011.

*Ph.D. Student, Institute of Metal Research, Shenyang National Laboratory for Materials Science; Graduate School of Chinese Academy of Sciences.

†Professor, Institute of Metal Research, Shenyang National Laboratory for Materials Science; mshli@imr.ac.cn (Corresponding Author).

‡Professor, Institute of Metal Research, Shenyang National Laboratory for Materials Science.

§Additional data available at http://www.matweb.com [accessed March 2011].

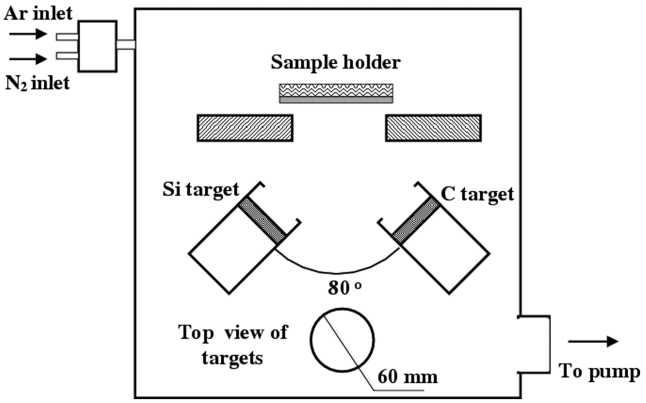

Fig. 1 Schematic illustration for the setup of sample and two targets during deposition of $Si_{1-x-y}C_xN_y$ coatings.

analysis, and the value of x and y was 0.43 and 0.31, respectively. Thus, the deposited coating was denoted as $Si_{0.26}C_{0.43}N_{0.31}$. Scanning electron microscope (SEM) observation indicated that pinholes appeared on the sample surface when the thickness of the $Si_{0.26}C_{0.43}N_{0.31}$ coating was less than 0.2 μm. However, the density of the pinholes decreased significantly with increasing the coating thickness. When the thickness increases to 0.7 μm, the pinholes on the coating surface have became undetectable. Therefore in this experiment, the coating with thickness of 0.7 μm was used for exposure tests due to its integrate and crack-free character.

The VUV/AO exposure tests were performed in a ground-based LEO simulation facility. Details about this system have been described elsewhere [16]. Briefly, a 2.45-GHz microwave source with a power of 500 W was launched into the circular cavity to generate electron convolution resonant (ECR) plasma. The oxygen ions were forced to a negatively biased Mo plate under the confining of a symmetrical magnetic mirror field, and then they were neutralized and reflected to form the AO beam. Meanwhile, a deuterium lamp with power of 30 W and wavelength of 114–200 nm was installed in the vacuum chamber of the facility to produce VUV radiation. The VUV intensity was about 0.4 W/(m^2nm), which is approximately 5–7 suns. In exposure experiment, the negatively biased voltage on the Mo plate was adjusted to produce a 5 eV-AO beam. According to our previous work, the reflected VUV intensity was significantly lower than the deuterium lamp-induced VUV intensity [17]. Therefore, the reflected VUV intensity could not affect the VUV exposure significantly.

The effective flux of the produced AO beam was calibrated by mass loss per unit area of a polyimide sample (marked as Kapton H), which is accepted as currently standard for measuring the total effective reactive particle fluence in space simulators. By comparing the mass loss generated during exposure in the simulator and the data obtained on orbital exposure, the AO flux can be determined. Apart from oxygen atoms, there may be other species existing in the produced beam, such as oxygen ions and oxygen molecules. The flux of oxygen ions in the AO beam was calibrated by a Langmuir probe, and its value was about 2 orders of magnitude lower than the corresponding AO flux. Therefore, the mass loss caused by oxygen ions is almost in negligible level, and previous studies on this kind of simulator indicated that the molecular oxygen exposure causes no apparent mass loss of polyimide sample [18].

Table 1 Deposition conditions of the $Si_{0.26}C_{0.43}N_{0.31}$ coating

Conditions	Values
Size of Si and C targets	Φ60 mm
Bias voltage	−120 V
Gas flow	Ar: N_2 = 20:10 (SCCM)
Working pressure	0.4 Pa
Base pressure	5×10^{-4} Pa
Power ratio of Si and C targets	90 W/70 W
Distance from each target to substrate	70 mm

In this study, the exposure tests were carried out in three conditions: exposure of VUV alone, exposure of AO alone, and simultaneous AO, VUV exposure (AO + VUV). The AO flux and VUV intensity were 4.5×10^{16} atoms/($cm^2 \cdot s$) and 5 suns, respectively.

During exposure, mass change of the as-deposited coatings was periodically weighted by electronic microbalance with a sensitivity of 10^{-5} g. Surface morphologies of the tested samples were observed by SEM and atomic force microscope (AFM). The surface chemical compositions of the samples were analyzed by XPS and Fourier transformed infrared spectroscopy (FTIR).

III. Results and Discussion

A. Erosion Kinetics

Figure 2 displays the mass change of the $Si_{0.26}C_{0.43}N_{0.31}$ coating during exposure in VUV, AO, and AO + VUV. It can be seen that exposure of VUV alone caused no mass loss of the sample. A further analysis of the exposed coating indicated that the surface morphology and compositions had no alternation. Thus, the exposure of VUV alone cannot induce erosion of the $Si_{0.26}C_{0.43}N_{0.31}$ coating. Details about the VUV effect would be discussed in Sec. III.D. During AO and AO + VUV exposure, the mass of the $Si_{0.26}C_{0.43}N_{0.31}$ coating decreased apparently, and the erosion kinetics almost followed a linear law in both conditions. The coating was eroded as a constant rate, which is denoted as the erosion yield. The erosion yield of the $Si_{0.26}C_{0.43}N_{0.31}$ coating was determined by the following equation:

$$E_y = \Delta M/(\rho A F t) \tag{1}$$

In the exposure period with total AO fluence of 3.2×10^{21} atoms/cm^2, the average E_y was 1.5×10^{-26} and 1.8×10^{-26} cm^3/atom in AO and AO + VUV exposure, respectively. The existence of VUV radiation caused an increase of 20% for the AO erosion yield. In any case, the E_y of the $Si_{0.26}C_{0.43}N_{0.31}$ coating was about 2 orders of magnitude lower than that of polyimide substrate (3.0×10^{-24} cm^3/atom). Therefore, the $Si_{0.26}C_{0.43}N_{0.31}$ coating could protect the polyimide substrate effectively from the attacks of AO as well as AO + VUV.

At the initial stage of AO or AO + VUV exposure, the incident oxygen atoms interacted with the $Si_{0.26}C_{0.43}N_{0.31}$ coating and an oxide-based layer formed on the coating surface. If only oxidation process had occurred, the rate of mass loss would have decreased with exposure time. But generally, the mechanism of AO erosion is proposed as bombardment-induced and -enhanced surface chemical etching. The bombardment of AO with high energy of about 5 eV also causes mass loss (etching effect). For example, a linear mass loss can be found on some AO inert oxide coatings, such as sol-gel Al_2O_3 and SiO_2 [19,20]. Because of the combining of oxidation induced "surface conversion layer" growth and etching induced "surface conversion layer" thinning, the AO erosion kinetics of the $Si_{0.26}$

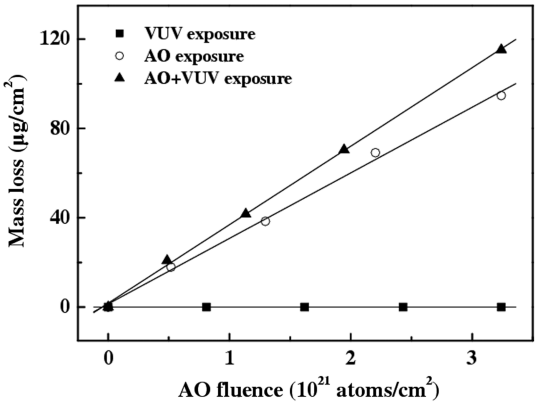

Fig. 2 Erosion kinetics of the $Si_{0.26}C_{0.43}N_{0.31}$ coating under AO and AO + VUV exposure AO flux = 4.5×10^{16} atoms/($cm^2 \cdot s$), VUV intensity = 5 suns.

$C_{0.43}N_{0.31}$ coating followed roughly a linear law, which means that the etching effect plays a remarkable role for the mass loss of the coating during exposure The formation of a hard oxide-rich top layer on the coatings can reduce AO etching and also retard the surface oxidation rate, which endows the coating the excellent AO erosion resistance. Indeed, the AO erosion yield of the $Si_{0.26}C_{0.43}N_{0.31}$ coating was determined to be in the same order with that of alumina or silica coatings [19,20].

Mass loss of the coated polyimide means that during exposures the $Si_{0.26}C_{0.43}N_{0.31}$ coating interacted with the incident oxygen atoms. The oxidation of $Si_{1-x-y}C_xN_y$ was proposed as follows:

$$Si_{1-x-y}C_xN_y + (2-x-y)O = (1-x-y)SiO_2 + xCO + yNO \quad (2)$$

$$CO + O = CO_2 \quad (3)$$

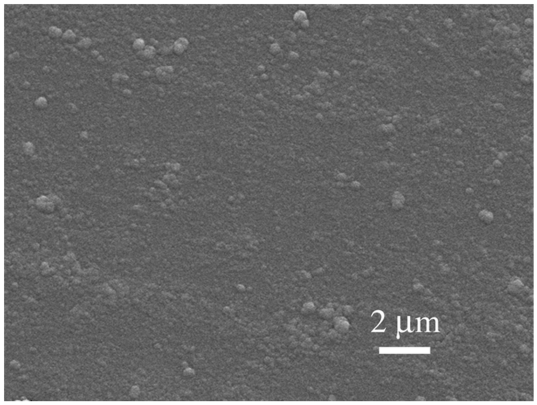

a)

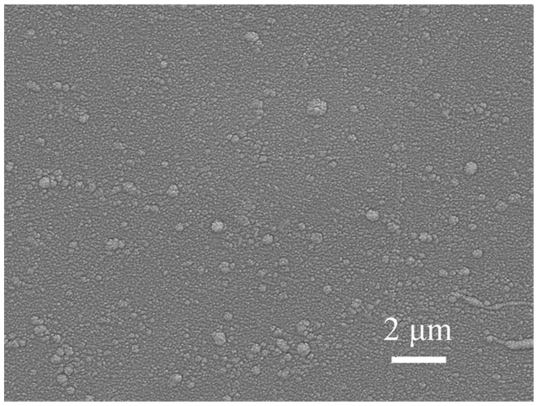

b)

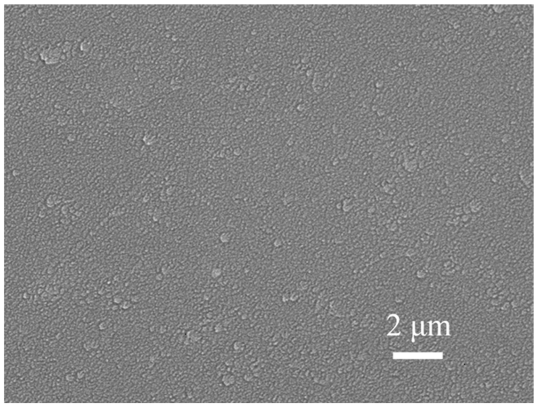

c)

Fig. 3 Surface micrographs of the $Si_{0.26}C_{0.43}N_{0.31}$ coating: a) before exposure, b) after AO exposure, and c) after AO + VUV exposure, AO fluence = 9.6 x 10^{20} atoms/($cm^2 \cdot s$)), VUV intensity = 5 suns.

For the $Si_{0.26}C_{0.43}N_{0.31}$, the calculation indicated that its mass decreased by 6.3% due to reaction (2) if it was oxidized completely, which is in agreement with our measured mass loss. Mass loss was also observed during the high temperature oxidation of $Si_{1-x-y}C_xN_y$ with the formation of a single layer of SiO_2 [12,15].

B. Surface Morphologies

Figure 3 shows the SEM images of the $Si_{0.26}C_{0.43}N_{0.31}$ coating before and after exposure. The surface of the as-deposited

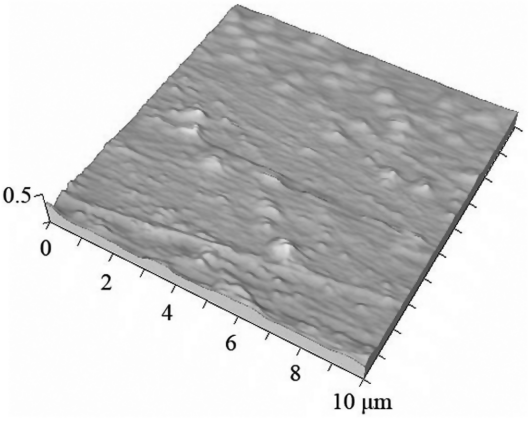

a)

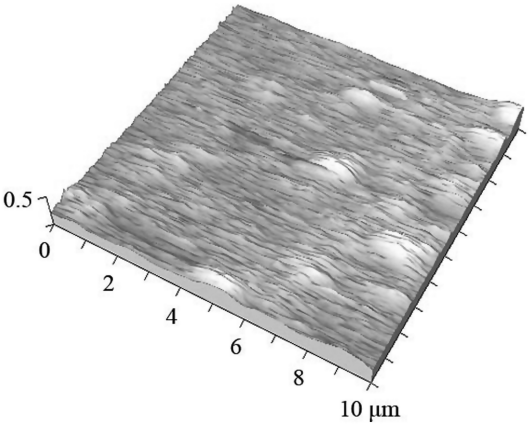

b)

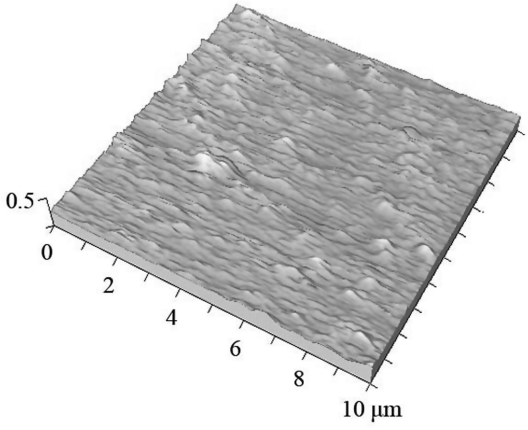

c)

Fig. 4 AFM images (10 μm x 10 μm, Z scale is 0.5 μm) of the $Si_{0.26}C_{0.43}N_{0.31}$ coating: a) unexposed, b) exposed to AO, and (c) exposed to AO + VUV, AO fluence = 9.6 x 10^{20} atoms/($cm^2 \cdot s$), VUV intensity = 5 suns.

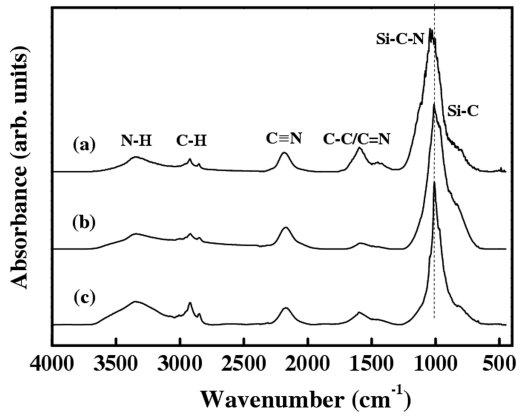

Fig. 5 FTIR spectra of the $Si_{0.26}C_{0.43}N_{0.31}$ coating: a) before exposure, b) after AO exposure, and c) after AO + VUV exposure, AO fluence = 3.2×10^{21} atoms/(cm^2 · s), VUV intensity = 5 suns.

$Si_{0.26}C_{0.43}N_{0.31}$ coating was smooth and crack free. After AO or AO + VUV exposure, the coating still kept its integrity, only its surface became a little rough. Thus, the $Si_{0.26}C_{0.43}N_{0.31}$ coating possessed good resistance to both AO and AO + VUV attacks. AFM was used to further investigate the evolution of surface morphology of $Si_{0.26}C_{0.43}N_{0.31}$ coating caused by exposures. The typical AFM images of the coating before and after exposure are shown in Fig. 4. It is clear that after either AO or AO + VUV exposure, a great number of bulges formed on the coating surface. The surface bulges were denser and smaller in AO + VUV exposure than those in single AO exposure. During AO exposure, the $Si_{0.26}C_{0.43}N_{0.31}$ coating was oxidized, its volume increased by about 2.5% due to the formation of SiO_2 as reaction (2) (it was assumed that SiO_2 was amorphous). Therefore, compressive stress was developed in the surface oxide layer, causing appearance of the rough surface morphology. During AO + VUV exposure, the reaction rate of the $Si_{0.26}C_{0.43}N_{0.31}$ coating with AO was a little higher; the surface roughness became more obvious.

C. Surface Compositions

FTIR spectra of the $Si_{0.26}C_{0.43}N_{0.31}$ coating before and after AO or AO + VUV exposure are presented in Fig. 5. All peaks centered at 2184 and 1043 cm^{-1} were characterized as C ≡ N and Si-C-N bonds, respectively [13]. The peak centered at 850 cm^{-1} was assigned to Si-C bonds. According to XPS analysis, the feature absorption at 1594 cm^{-1} was associated with C = N or C-C bonds. As shown in Fig. 5, the absorption intensity of C ≡ N peak displayed only a little difference after exposure in AO and AO + VUV, indicating that C ≡ N bonds had a good stability in simulated environments. On the contrary, the intensity of C = N/C-C bonds decreased remarkably after both AO and AO + VUV exposure. These bonds were not stable in simulated environments, and might have broken during exposures. After AO exposure, the peak of Si-C-N exhibited narrower width with a little shift to a lower wavenumber. The intensity of Si-C bonds (around 850 cm^{-1}) became stronger. After AO + VUV exposure, the width of Si-C-N peak and the intensity of Si-C peak became smaller compared with that after single AO exposure. Obviously, the breakage of Si-C-N and Si-C bonds was more severe in AO + VUV exposure. The peak shift of Si-C-N might be induced by the breakage of Si-N bonds (they had a little higher wavenumber than Si-C-N) and formation of Si-C-O bonds (they had a little lower wavenumber than Si-C-N). Obviously, VUV radiation could enhance the bonds breakage in the $Si_{0.26}C_{0.43}N_{0.31}$ during AO + VUV exposure.

Surface compositions of the $Si_{0.26}C_{0.43}N_{0.31}$ coating before and after AO, AO + VUV exposure were investigated by XPS using a monolithic Al-K_α excitation radiation, and the obtained data are summarized in Table 2. Detected O element on the unexposed coating was induced by O_2 adsorption, which can be identified by a further analysis of O1s high-resolution spectra. After AO and AO + VUV exposure, the concentration of C varied from 34.01 to 27.18 and 35.18%, while the O-to-Si ratio increased from 0.18 to 1.95 and 2.05, respectively. Therefore, it was reasonable to propose that a protective SiO_2-rich layer formed on the coating surface after exposures in AO and AO + VUV. And the C and N species interacted with oxygen atoms to form volatile gases of NO, CO, and CO_2, as proposed in reactions (2) and (3).

Table 2 Surface compositions of $Si_{0.26}C_{0.43}N_{0.31}$ coating before and after exposures, AO fluence = 3.2×10^{21} atoms/(cm^2 · s), VUV intensity = 5 suns

Coating	Composition, %				Atomic ratio
	Si	C	N	O	O/Si
Unexposed	25.05	41.24	29.09	4.62	0.18
AO exposed	24.65	27.18	—	48.17	1.94
AO + VUV exposed	21.22	35.18	—	43.60	2.05

High-resolution XPS spectra of Si2p obtained on the surface of the $Si_{0.26}C_{0.43}N_{0.31}$ coating are shown in Fig. 6. Variations in peak shapes and positions were observed on the exposed surfaces, indicating that the distribution of chemical species had been altered. The peak of Si2p became narrow after AO and AO + VUV exposure, implying that a unique layer formed on the surface of the exposed $Si_{0.26}C_{0.43}N_{0.31}$ coating. Before exposure, the Si2p had a binding energy (BE) of 101.65 eV, which is close to the BE of Si-N bond (101.5 eV). After AO and AO + VUV exposure, the peak of Si2p shifted about 1 eV to a higher BE and centered at 102.65 eV and 102.60 eV, respectively, which corresponded to amorphous SiO_2 (102.7 eV). It should be noted that a part from SiO_2, other kinds of SiO_x ($X = 0.5$,1.0 and 1.5) might form on the coating surface. Thus, the high-resolution O1s also has been analyzed; only one main peak without any other fitting peaks appeared, indicating that SiO_2 is the exclusive oxide. Again, it is concluded that a SiO_2-rich layer formed on the coating surface after either AO or AO + VUV exposure. The formation of this SiO_2-rich layer played a main role in preventing further erosion of the underlying. On the other hand, the deconvolution of Si2p indicated that the exposed surface of the $Si_{0.26}C_{0.43}N_{0.31}$ coating was composed of Si-N and Si-O bonds. After exposure to AO + VUV, the calculated intensity ratio of Si-N/Si-O on the exposed surface decreased from 0.44 to 0.39. Therefore, N-related bonds broke more severely under AO + VUV exposure.

D. Effects of VUV Radiation During AO Exposure

According to the above erosion kinetic data, it is obvious that the evolution of mass loss of the $Si_{0.26}C_{0.43}N_{0.31}$ coating followed a linear law, and the existence of VUV could enhance the attacks of AO. It can be known by comparing the data in Table 2 and Fig. 6 that the

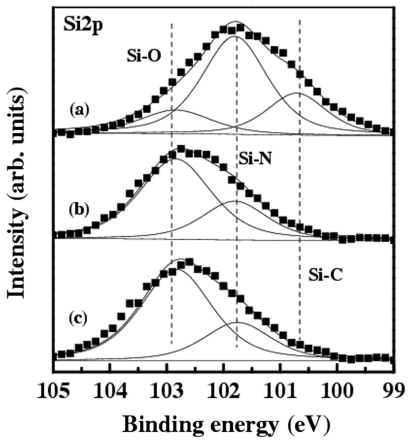

Fig. 6 High-resolution XPS spectra of Si2p of the $Si_{0.26}C_{0.43}N_{0.31}$ coating: a) before exposure, b) after AO exposure, and c) after AO + VUV exposure, AO fluence = 3.2×10^{21} atoms/(cm^2 · s), VUV intensity = 5 suns.

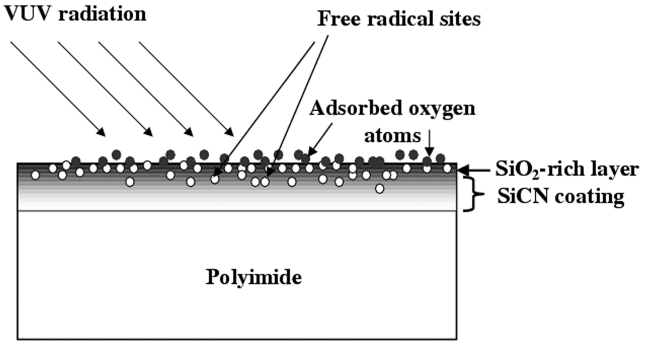

Fig. 7 Schematic illustration for the erosion process of the $Si_{0.26}C_{0.43}N_{0.31}$ coating under AO + VUV exposure.

concentration of C was higher, and the peak of Si2p was wider in AO + VUV exposure than in AO exposure. These results may provide clues for explaining the VUV effects on AO erosion of the $Si_{0.26}C_{0.43}N_{0.31}$.

The mechanism of AO erosion was proposed as bombardment-induced and -enhanced surface chemical etching [21]. During single AO exposure, the oxygen atoms absorbed on the surface at the initial stage, then these absorbed oxygen atoms interacted with N and C in $Si_{0.26}C_{0.43}N_{0.31}$ simultaneously, gaseous products such as NO, CO, and CO_2 released into the simulated environment, and finally a continuous SiO_2-rich layer formed. The oxidation process could be described as the following reactions (4–7):

$$\mathrm{Si}_{1-x-y}\mathrm{C}_x\mathrm{N}_y + (1+y)\mathrm{O} = \mathrm{Si}_{1-x-y}\mathrm{C}_x\mathrm{O} + y\mathrm{NO} \quad (4)$$

$$\mathrm{Si}_{1-x-y}\mathrm{C}_x\mathrm{N}_y + (1+x)\mathrm{O} = \mathrm{Si}_{1-x-y}\mathrm{ON}_y + x\mathrm{CO} \quad (5)$$

$$\mathrm{Si}_{1-x-y}\mathrm{C}_x\mathrm{O} + \mathrm{O} = \mathrm{SiO}_2 + y\mathrm{CO} \quad (6)$$

$$\mathrm{Si}_{1-x-y}\mathrm{ON}_y + \mathrm{O} = \mathrm{SiO}_2 + x\mathrm{NO} \quad (7)$$

During AO + VUV exposure, an essential similar process occurred. However, VUV radiation might break those chemical bonds with low binding energy [22], such as C-N, C-C, created a great number of free radical sites [22] on the $Si_{0.26}C_{0.43}N_{0.31}$ surface. Because the interaction of AO occurred easily at these free radical sites, the erosion rate of AO increased under the existence of VUV. The erosion process of the $Si_{0.26}C_{0.43}N_{0.31}$ coating is exhibited schematically in Fig. 7. Moreover, the N-related bonds were more susceptible to VUV radiation than corresponding C related bonds [23]. Under AO + VUV exposure, the reactions (4) and (7) occurred more preferentially than the reactions (5) and (6), because only these two reactions are involved in the breakage of Si-N bonds to form NO (otherwise to form CO). Hence, after AO + VUV exposure, more Si-C-O species existed on the coating surface, which resulted in the raising of the C concentration and widening of Si2p peak.

IV. Conclusions

Amorphous $Si_{0.26}C_{0.43}N_{0.31}$ coating was deposited on polyimide substrate by reactive magnetron cosputtering Si and C targets, and the AO resistance of $Si_{0.26}C_{0.43}N_{0.31}$ coating was evaluated in a ground-based LEO environment simulation facility. Through the experimental studies, the following conclusions can be drawn:

1) The erosion yield of the $Si_{0.26}C_{0.43}N_{0.31}$ coating was 1.5× and 1.8×10^{-26} cm^3/atom during exposures in AO and AO + VUV, respectively, being about 2 orders of magnitude lower than that of polyimide. The existence of VUV could enhance AO erosion definitively.

2) During AO and AO + VUV exposure of the $Si_{0.26}C_{0.43}N_{0.31}$ coating, gaseous products of CO, CO_2, and NO generated, and an oxidized layer composed of SiO_2 and minor Si-C-O formed, which rendered the $Si_{0.26}C_{0.43}N_{0.31}$ coating good erosion resistance.

3) VUV radiation might promote the breakage of those chemical bonds with low binding energy, especially N-related bonds such as C-N and C = N, creating free radical sites easily on the $Si_{0.26}C_{0.43}N_{0.31}$ surface.

Acknowledgment

This work was supported by Chinese Academy of Sciences.

References

[1] Hansen, R. H., Pascale, J. V., De Benedictis, J., and Rentzepis, P. M., "Effects of Atomic Oxygen on Polymers," *Journal of Polymer Science*, Part A, Vol. 3, June 1965, pp. 2205–2214.

[2] Bank, B. A., Rutledge, S. K., Brady, J. A., and Merrow, J. E., "Atomic Oxygen Effects on Materials," *Proceedings of the NASA/SDIO Space Environment effects on Materials Workshop*, edited by L. Teichman, and B. A. Stein, NASA CP 3035, Vol. 1, June 1988.

[3] Arnold, G. S., and Peplinski, D. R., "Reaction of Atomic Oxygen with Polyimide Films," *AIAA Journal*, Vol. 23, No. 10, 1985, pp. 1621–1626.
doi:10.2514/3.9133

[4] Koontz, S. L., Leger, L., and Albyn, K., "Vacuum Ultraviolet Radiation/Atomic Oxygen Synergism in Materials Reactivity," *Journal of Spacecraft and Rockets*, Vol. 27, No. 3, 1990, pp. 346–348.
doi:10.2514/3.26146

[5] Tagawa, M., Yokota, K., and Ohmae, N., "Synergistic Study on Atomic Oxygen-Induced Erosion of Polyethylene with Vacuum Ultraviolet," *Journal of Spacecraft and Rockets*, Vol. 41, No. 3, 2004, pp. 345–349.
doi:10.2514/1.10888

[6] Ghosh, L., Fadhilah, M. H., Kinoshita, H., and Ohmae, N., "Synergistic Effects of Hyperthermal Atomic Oxygen Beam and Vacuum Ultraviolet Radiation Exposures on the Mechanical Degradation of High-Modulus Aramid Fibers," *Polymer*, Vol. 47, No. 19, 2006, pp. 6836–6842.
doi:10.1016/j.polymer.2006.07.029

[7] Raddy, M. R., "Review: Effects of Low Earth Orbit Atomic Oxygen on Spacecraft Materials," *Journal of Materials Science*, Vol. 30, No. 2, 1995, pp. 281–307.
doi:10.1007/BF00354389

[8] Tennyson, R. C., "Protective Coatings for Spacecraft Materials," *Surface and Coatings Technology*, Vols. 68–69, 1994, pp. 519–527.
doi:10.1016/0257-8972(94)90211-9

[9] David, P. D., and Mark, D. S., "Protective Space Coatings: a Ceramer Approach for Nanoscale Materials," *Progress in Organic Coatings*, Vol. 47, 2003, pp. 448–457.
doi:10.1016/s0300-9440(03)00135-8

[10] Tuman, S. J., Chamberlain, D., Scholsky, K. M., and Soucek, M. D., "Differential Scanning Calorimetry Study of Linseed Oil Cured with Metal Catalysts," *Progress in Organic Coatings*, Vol. 28, 1996, pp. 251–258.

[11] Li, J., Luo, R. Y., Lin, C., Bi, Y. H., and Qiao, X., "Oxidation Resistance of a Gradient Self-Healing Coating for Carbon/Carbon Composites," *Carbon*, Vol. 45, No. 13, 2007, pp. 2471–2478.
doi:10.1016/j.carbon.2007.08.036

[12] Wang, Y. H., Moitreyee, M. R., and Kumar, R., "A Comparative Study of Low Dieletric Constant Barrier Layer, Etch Stop and Handmask Films of Hydrogenated Amorphous Si-(C, O, N)," *Thin Sold Films*, Vol. 460, Nos. 1–2, 2004, pp. 211–216.
doi:10.1016/j.tsf.2004.01.055

[13] Chen, L. C., Chen, K. H., Wei, S. L., Kichambare, P. D., Wu, J. J., Lu, T. R., and Kuo, C. T., "Crystal SiCN: a Hard Material Rivals to Cubic BN," *Thin Solid Films*, Vol. 355, No. 1, 1999, pp. 112–116.
doi:10.1016/S0040-6090(99)00490-3

[14] Liew, L. A., Zhang, W. G., Bright, V. M., An, L. N., Dunn, M. L., and Raj, R., "Fabrication of SiCN Ceramic MEMS Using Injectable Polymer-Precursor," *Sensors and Actuators A-Physical*, Vol. 89, Nos. 1–2, 2001, pp. 64–70.
doi:10.1016/S0924-4247(00)00545-8.

[15] Berlind, T., Hellgren, N., Johansson, M. P., and Hultman, L., "Microstructure, Mechanical Properties, and Wetting Behavior of Si-C-N Thin Films Grown by Reactive Magnetron Sputtering," *Surface and Coatings Technology*, Vol. 141, Nos. 2–3, 2001, pp. 145–155.
doi:10.1016/S0257-8972(01)01236-1

[16] Duo, S. W., Li, M. S., and Zhang, Y. M., "A Simulator for Producing of High Flux Atomic Oxygen Beam by Using ECR Plasma Source," *Journal of Materials Science and Technology (Shenyang, People's*

Republic of China), Vol. 20, No. 6, 2004, pp. 759–762.

[17] Hu, L. F., Li, M. S., and Zhou, Y. C., "Effects of Vacuum Ultraviolet Radiation on Atomic Oxygen Erosion of Polysiloxane/SiO_2 Hybrid Coatings," *Journal of Materials Science and Technology*, Vol. 25, No. 4, 2009, pp. 483–488.

[18] Leger, L. J., Koontz, S. L., Visentine, J. T., and Cross, J. B., "Laboratory Investigations Involving High-Velocity Oxygen Atoms," *Fourth International symposium on Spacecraft Materials in the Space Environment*, ONERA-Centre d'Etudes et de Recherches de Toulouse, Cėdex, France, Sept. 1988.

[19] Zhang, X., Wu, Y. Y., Liu, G., He, S. Y., and Yang, D. Z., "Investigation on Sol-Gel Boehmite-AlOOH Films on Kapton and Their Erosion Resistance to Atomic Oxygen," *Thin Solid Films*, Vol. 516, No. 15, 2008, pp. 5020–5026. doi:10.1016/j.tsf.2008.01.023

[20] Zhang, X., Wu, Y. Y., He, S. Y., Yang, D. Z., and Li, F., "Investigation on the Atomic Oxygen Erosion Resistance of Surface Sol-Gel Silica Films," *Surface and Coatings Technology*, Vol. 202, No. 15, 2008, pp. 3464–3469. doi:10.1016/j.surfcoat.2007.12.022

[21] Iskanderova, Z. A., Kleiman, J. I., Gudimenko, Yu., and Tennyson, R. C., "Influence of Content and Structure of Hydrocarbon Polymers on Erosion by Atomic Oxygen," *Journal of Spacecraft and Rockets*, Vol. 32, No. 5, 1995, pp. 878–884. doi:10.2514/3.26699

[22] Slemp, W. S., "Ultraviolet Radiation Effects," *NASA/SDIO Space Environment Effects on Materials Workshop*, NASA CP 3035, Part 2, 1989, pp. 425–446.

[23] Silverman, E. M., "Space Environmental Effects on spacecraft: LEO Materials Selection Guide," NASA CP 4661, Pt. 1, 2005, pp. 22–24.

T. Minton
Associate Editor